Original Full Length Article

Modulation of endochondral ossification by MEK inhibitors PD0325901 and AZD6244 (Selumetinib)

J. El-Hoss [a,b], M. Kolind [a], M.T. Jackson [c], N. Deo [a,b], K. Mikulec [a], M.M. McDonald [d], C.B. Little [c], D.G. Little [a,b], A. Schindeler [a,b,]*

[a] Orthopaedic Research & Biotechnology Unit, The Children's Hospital at Westmead, Sydney, Australia
[b] Discipline of Paediatrics and Child Health, Faculty of Medicine, University of Sydney, Sydney, Australia
[c] Raymond Purves Bone and Joint Research Laboratories, Kolling Institute of Medical Research, University of Sydney, Royal North Shore Hospital, Sydney, Australia
[d] Bone Biology Group, Garvan Institute for Medical Research, Sydney, Australia

ARTICLE INFO

ABSTRACT

MEK inhibitors (MEKi) PD0325901 and AZD6244 (Selumetinib) are drugs currently under clinical investigation for cancer treatment, however the Ras–MAPK pathway is also an important mediator of normal bone cell differentiation and function. In this study we examined the effects of these compounds on endochondral processes using both *in vitro* and *in vivo* models. Treatment with PD0325901 or AZD6244 significantly increased *Runx2* and *Alkaline phosphate* gene expression in calvarial osteoblasts and decreased TRAP+ cells in induced osteoclast cultures. To test the effects of these drugs on bone healing, C57/Bl6 mice underwent a closed tibial fracture and were treated with PD0325901 or AZD6244 at 10 mg/kg/day. Animals were culled at day 10 and at day 21 post-fracture for analysis of the fracture callus and the femoral growth plate in the contralateral leg. MEKi treatment markedly increased cartilage volume in the soft callus at day 10 post-fracture (+60% PD0325901, +20% AZD6244) and continued treatment led to a delay in cartilage remodeling. At the growth plate, we observed an increase in the height of the hypertrophic zone relative to the proliferative zone of +78% in PD0325901 treated mice. Osteoclast surface was significantly decreased both at the terminal end of the growth plate and within the fracture calluses of MEKi treated animals. The mechanistic effects of MEKi on genes encoding cartilage matrix proteins and catabolic enzymes were examined in articular chondrocyte cultures. PD0325901 or AZD6244 led to increased matrix protein expression (*Col2a1* and *Acan*) and decreased expression of catabolic factors (*Mmp13* and *Adamts-5*). Taken together, these data support the hypothesis that MEKi treatment can impact chondrocyte hypertrophy, matrix resorption, and fracture healing. These compounds can also affect bone architecture by expanding the hypertrophic zone of the growth plate and reducing osteoclast surface systemically.

Crown Copyright © 2013 Published by Elsevier Inc. All rights reserved.

Introduction

The Ras signaling molecule is an important mediator of cell survival, proliferation and function. The Ras–Raf–MEK–ERK axis (also called the Ras–MAPK pathway) has a central role in cell signaling, and is activated in many human cancers [1]. Activating mutations in the Ras superfamily have been identified in approximately 15% of all human cancers, while B-Raf mutations affect a number of tissue specific cancers [2]. MEK plays a key role in transducing these upstream signals, and has thus been a highly studied therapeutic target.

MEK inhibitors (MEKi) PD0325901 (Pfizer) and AZD6244 (Selumetinib, ARRY-142886, AstraZeneca) are small molecule drugs that can reduce tumor growth in preclinical xenograft models [3–6].

These compounds are undergoing clinical trials for treatment of a variety of tumor types with PD0325901 being used for advanced stage cancers (Trial ID: NCT01347866), and AZD6244 being used in over 50 trials in oncology patients. To date, the adverse effect profile has been limited to nausea, edema, skin rashes, visual disturbances, fatigue and diarrhea, which have been manageable and dose dependent [7]. The development of specific and bioavailable MEKi compounds AZD6244 (Selumetinib) and PD0325901 provides a unique opportunity to explore the role of MEK signaling in skeletal biology. The potential impact of MEKi in bone is of particular relevance to cancer patients as these treatments can lead to bone loss and increased fracture risk [8,9]. In breast cancer patients without bone metastasis or MEKi treatment, the incidence of vertebral fractures was 5 fold greater than the normal population. In women with recurrent breast cancer, the risk was 20 fold greater than normal [9]. As these drugs progress through clinical development, a better understanding of their skeletal manifestation is important. Three registered clinical trials are focused on pediatric patients, yet limited information is available regarding the role of MEKi on the developing skeleton, skeletal homeostasis, and bone repair.

* Corresponding author at: Orthopaedic Research & Biotechnology, Research Building, The Children's Hospital at Westmead, Locked Bag 4001, Westmead, NSW 2145, Australia. Tel.: +61 2 98451451; fax: +61-2-98453078.
E-mail address: aaron.schindeler@sydney.edu.au (A. Schindeler).

A *ALP* expression in calvarial osteoblasts treated with MEKi

B *Runx2* expression in calvarial osteoblasts treated with MEKi

C Mineralised nodules in MEKi treated calvarial osteblasts in culture

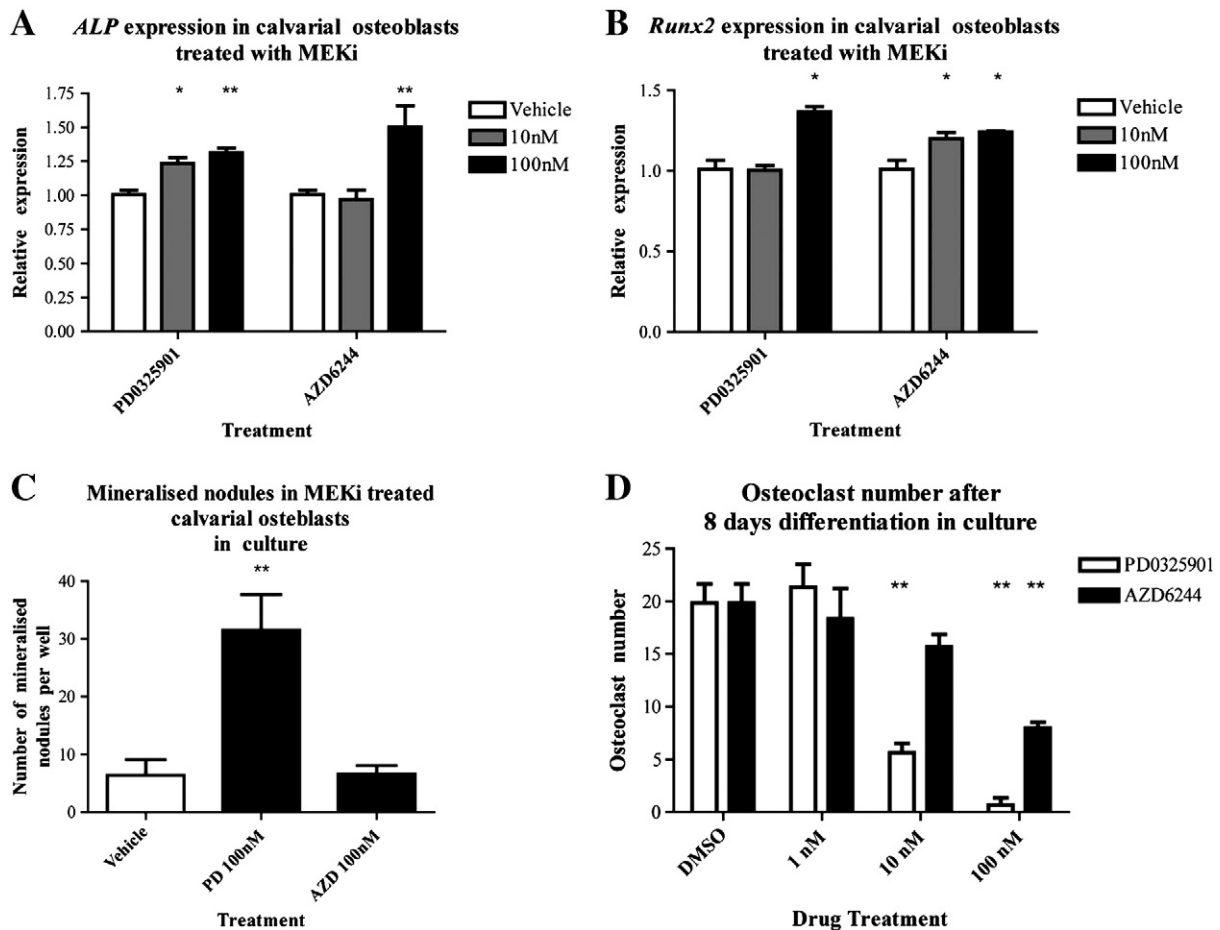**D** Osteoclast number after 8 days differentiation in culture

Fig. 1. MEK inhibition in calvarial osteoblasts and bone marrow derived osteoclasts. Calvarial osteoblasts were differentiated with rhBMP2 (100 ng/ml) and PD0325901 or AZD6244. RNA was harvested at day 9 and expression of *Alkaline phosphatase* and *Runx2* was quantified (A, B). Cells were then stained with Alizarin Red S for mineral and quantified (C). MEKi treatment led to an increase in osteogenic potential. Bone marrow osteoclasts were differentiated using M-CSF and RANKL and co-treated with PD0325901 or AZD6244 for 8 days (D). A TRAP stain for osteoclasts revealed that MEKi treatment reduced osteoclast numbers in the well. ($^*p < 0.05$, $^{**}p < 0.01$, ANOVA).

Endochondral ossification is a key process involved with both skeletal development and repair. During development, mesenchymal progenitors are recruited and condense to differentiate into pre-chondrocytes. Differentiation of pre-chondrocytes to chondrocytes is regulated by the master regulator gene *Sox9*, in addition to *Sox4* and *Sox5* [10,11]. During this early phase of differentiation, chondrocytes express collagen type I (*Col1a1*), and then secrete increasing amounts of collage type II (*Col2a1*) and aggrecan (*Acan*) [11]. As chondrocytes continue through the cell cycle, they begin to organize into columns of proliferating chondrocytes, and eventually enter the terminal phase of differentiation and become hypertrophic chondrocytes [10]. Hypertrophic chondrocytes secrete high levels of collagen type X (*Col10a1*), vascular endothelial growth factor (*Vegf*), and in the final stages of differentiation, matrix metalloproteinase 13 (*Mmp13*) [11]. The expression of *Mmp13* and *Vegf* promote cartilage remodeling and invasion of vessels that enable infiltration of osteoblasts and osteoclasts. In the final stages of endochondral ossification, the invasion of bone cells replaces the cartilage with stronger trabecular bone.

Endochondral ossification is a fundamental process that occurs during development at the growth plates of all long bones, and contributes to bone lengthening. This process is also recapitulated during fracture
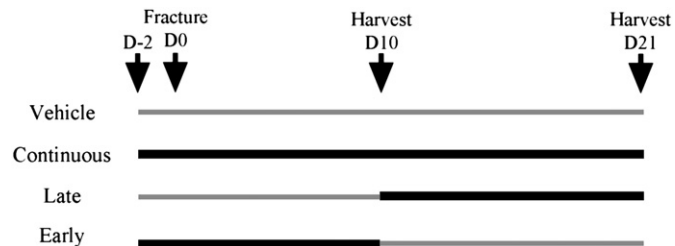
Fig. 2. Experimental design for targeted MEK inhibition during fracture healing. Mice were treated with PD0325901 or AZD6244 at 10 mg/kg/day and assigned to one of the above groups. Mice were treated continuously from days −2 to 21 post fracture with a MEKi (black bar), or received vehicle treatment for the duration of the experiment (gray bar). To determine the effects of the drugs on the different stages of healing, separate mice were also treated from day −2 pre-fracture to day 10 post fracture (Early group), or from day 10 to day 21 post fracture (Late group). Mice from all groups were sacrificed at day 10 and 21 post-fracture for analysis.

Table 1
MicroCT analysis of MEKi treatments at 21 days post-fracture.

Study — treatment	Mineralized volume (um³)	Tissue volume (um³)	% MV/TV
Study 1 — PD0325901			
Vehicle	7.35 (0.56)	23.48 (1.98)	31.59 (0.79)
Continuous	9.08 (0.92)	23.29 (2.53)	39.20** (0.63)
Late	9.34 (0.57)	26.63 (2.46)	36.29* (1.90)
Early	7.29 (0.44)	19.61 (1.18)	37.48** (1.39)
Study 2 — AZD6244			
Vehicle	5.40 (0.22)	14.05 (0.96)	39.13 (1.23)
Continuous	4.17** (0.27)	9.66** (0.98)	45.06* (2.18)
Late	4.25** (0.21)	10.12** (0.70)	42.56 (1.50)
Early	4.31** (0.23)	10.36* (0.77)	42.25 (1.38)

* $p < 0.05$, one-way ANOVA with Dunnett's post-test. N = 9–10.
** $p < 0.01$, one-way ANOVA with Dunnett's post-test. N = 9–10.

A
**Cartilage tissue in fracture callus
10 days post fracture
with PD0325901**

B
**Cartilage tissue in fracture callus
10 days post fracture
with AZD6244**

C
**Cartilage tissue in fracture callus
21 days post fracture
with PD0325901**

D
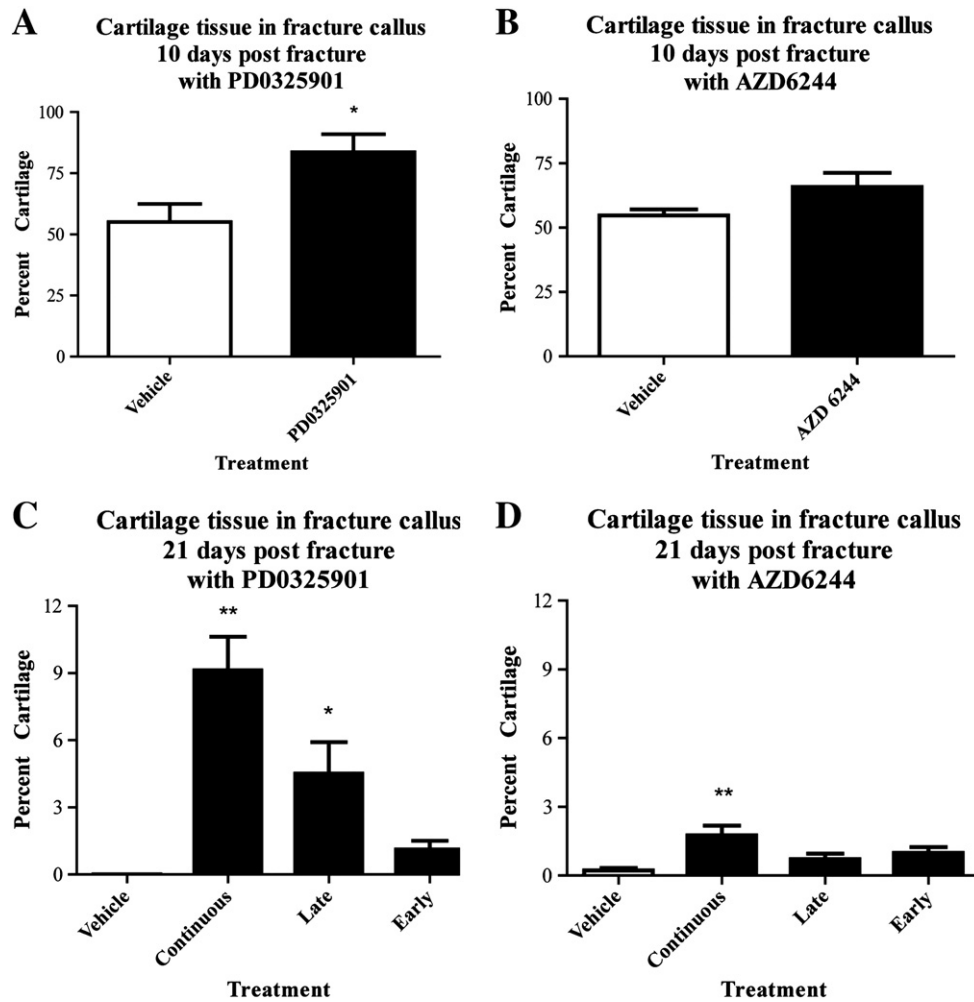**Cartilage tissue in fracture callus
21 days post fracture
with AZD6244**

Fig. 3. Cartilage formation in fracture calluses of MEKi-treated mice. C57/Bl6 mice were treated with PD0325901 or AZD6244 as defined in Fig. 2 and underwent a closed fracture surgery to assess healing dynamics. Mice were harvested at day 10 (A, B) or day 21 (C, D) post-fracture and cartilage area was quantified histologically. PD0325901 significantly increased cartilage formation at day 10 (A). Continuous treatment with a MEKi led to more cartilage at day 21 (C, D), while stopping at day 10 led to cartilage resorption by day 21 (Early group). Starting MEKi treatment at day 10 (Late group) resulted in maintenance of cartilage at day 21 (C, D). (N = 3–10, *$p < 0.05$, **$p < 0.01$, ANOVA).

healing [12]. Fracture healing follows a sequential series of events: the initial inflammatory reaction, the development of a cartilaginous soft callus, followed by laying down of trabecular bone of the hard callus (by endochondral ossification), finally, the trabecular bone is remodeled into stronger lamellar bone that takes the shape of the original bone [13]. In mice, the cartilage of the soft callus peaks at about 10 days, and the trabecular bone of the hard callus peaks at about 21 days post fracture [12,13].

Genetic mouse models have demonstrated the importance of the Ras–MAPK pathway in chondrocyte and osteoblast cell differentiation and function. Transgenic mice with inactivating or overactive mutations of MEK driven by the *osteocalcin* promoter have yielded important insights [14]. These studies intimated an important role for MEK in promoting the bone forming activity of late stage osteoblasts where *osteocalcin* is expressed. In contrast, inactivation of ERK1/2 (the downstream targets of MEK) using the *Prx1* promoter (expressed in mesenchymal progenitors of the limb) promoted chondrogenesis at the expense of osteogenesis [15]. Intriguingly, this mouse model showed decreased RANKL expression in the humerus and tibia, indicating decreased resorptive signaling. Furthermore, animal studies have identified that ERK is highly expressed in hypertrophic chondrocytes, suggesting an important regulatory role [16]. Taken together, these studies suggest that the Ras–MAPK pathway has an important role in the specification and differentiation of osteochondral progenitors as well as the function of mature osteoblasts.

In this study we have evaluated the impact of AZD6244 and PD0325901 on cultured cells, fracture healing, and in the growth plates of mice. MEKi treatments were applied *in vitro* to osteoblasts, chondrocytes, and osteoclasts. To address the role of MEK inhibition on bone repair, mice underwent closed fracture surgery and were treated with PD0325901 and AZD6244 at 10 mg/kg/day using several dosing regimens. Fracture specimens were analyzed by microCT and tissue histology. To determine how these compounds may impact bone growth, the growth plates of contralateral limbs were also analyzed. Biochemical markers for bone turnover were also assessed.

Materials and methods

Calvarial osteoblast cultures

Calvarial cultures were generated from neonatal mice harvested within one week of birth as previously published [17]. Briefly, mice were decapitated and the calvaria were washed in Dulbecco's PBS while stripping any remaining fibrous tissue. Calvaria were minced and digested three times in Collagenase D at 1 mg/ml (Roche) in αMEM (Invitrogen) at 37 °C for 15 min per digestion. The resulting calvaria fragments were plated in 10% fetal bovine serum in αMEM with penicillin/streptomycin and cells were allowed 3–5 days to grow onto the plate before splitting for experiments. At confluence, cultures were differentiated with α-MEM containing 10% FBS and penicillin/
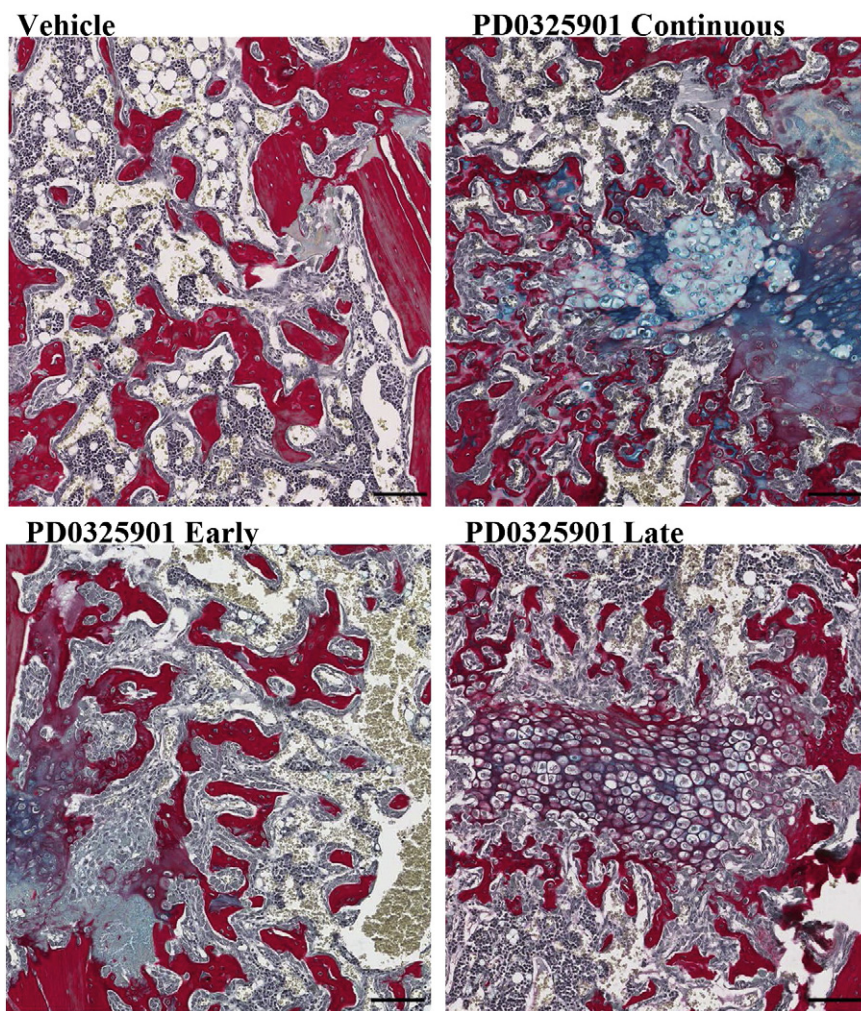
Vehicle

PD0325901 Continuous

PD0325901 Early

PD0325901 Late

Fig. 4. Histology of fracture callus at day 21 post-fracture in MEKi treated mice. C57/Bl6 mice were treated with PD0325901 orally at 10 mg/kg. Mice were assigned to four groups as defined in Fig. 2. Mice were harvested at day 21 for histological analysis. Picrosirius Red/Alcian Blue stain revealed cartilage area in blue and Collagen I (bone) in red. Vehicle control samples showed complete bony union with no cartilage callus present at this point. Continuous treatment led to cartilage islands, while the Early group had mostly resorbed, and the Late group showed hypertrophic chondrocytes in the PD0325901 group.

streptomycin, supplemented with 10 mM β-glycerophosphate, 50 μg/ml ascorbic acid, and 100 ng/ml of rhBMP-2 (Medtronic Australasia). PD0325901 was dissolved in DMSO and added to the differentiation media.

Induction of mineralization was established by staining for calcium deposits in the well. Cells were fixed with 4% paraformaldehyde for 10 min, followed by 5 minute incubation with Alizarin Red S (40 mM, pH 4.2). Samples were washed three times with water and mineralization nodules were quantified using a light microscope.

To examine osteogenesis, quantitative PCR was performed on a Rotorgene LightCycler. RNA was harvested from cells using Trizol Reagent (Invitrogen), and cDNA using Superscript III (Invitrogen). qPCR was performed using a SYBR Green Mastermix (Stratagene) using the following primer sequences: ALP-F 5′-GGGACTGGTACTCGGATAACGA-3′, ALP-R 5′-CTGATATGCGATGTCCTTGCA-3′; Runx2-F 5′-AGCCTCTTCA GCGCAGTGAC–Runx2-R 5′-CTGGTGCTGCGATCCCAA. Dissociation curves using these primer pairs resulted in a single amplification peak, confirming the specificity of these primers.

Osteoclast cultures

Bone marrow was harvested from the femur of C57/Bl6 mice aged to 8–10 weeks. The bone marrow suspension was filtered using a 40 μm filter, washed in PBS, and resuspended in DMEM with 10% FBS and antibiotics. M-CSF (20 ng/ml; R&D Systems, MN, USA) and RANKL (100 ng/ml; R&D Systems, MN, USA) were used to differentiate the cells towards the osteoclastic lineage, and PD0325901 or AZD6244 were co-delivered as appropriate in the media. Cells were incubated and differentiated for 8 days before performing a TRAP stain to assess osteoclast numbers in the well as previously described.

Surgical methods

Female C57Bl6 mice aged ~11 weeks were used in closed fracture surgery experiments. All fractures were generated at the tibial midshaft (near the fibular junction) by experienced staff based on our published methodology [18]. Anesthesia was induced with ketamine (35 mg/kg) and xylazine (4.5 mg/kg) *via* intraperitoneal injection with a 27-G needle and maintained using inhaled isoflurane. Next a small incision was made slightly below the knee and an entry point made using a 27-G needle. An intramedullary rod (a 30-G needle or a 0.3 mm-diameter stainless steel insect pin) was surgically inserted inside the medullary canal of the tibia, and a second pin inserted for stability. A non-comminuted, transverse fracture near the fibular junction was confirmed *via* radiography using a digital X-ray machine (Faxitron X-ray Corp., Wheeling, IL). The wound was closed using 5–0 nylon suture (Ethicon Inc., Somerville, NJ). The mice were allowed to recover on a heated pad and then placed in recovery cages. Pain was managed using buprenorphine (0.05 mg/kg subcutaneously postoperatively, then every 12 h as required) and dehydration
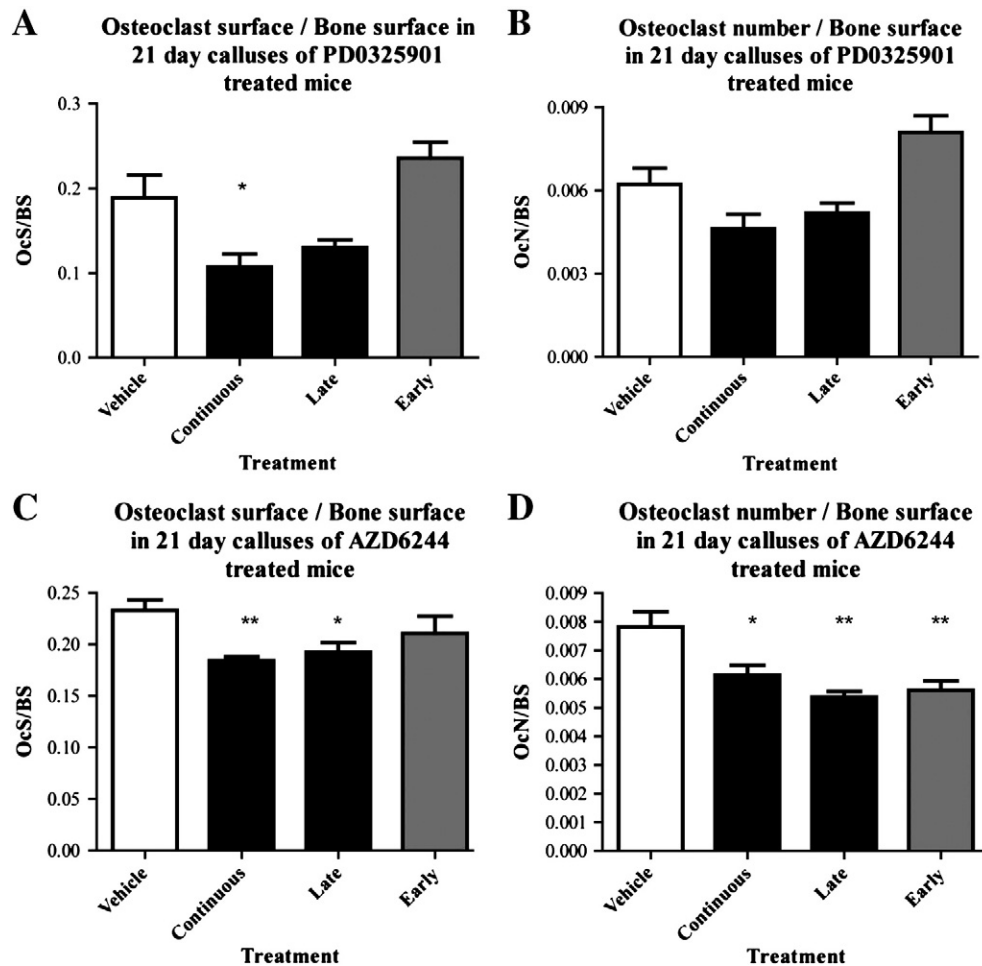
Fig. 5. Osteoclast parameters in fracture callus at 21 days of MEKi treated mice. Mice were grouped as described in Fig. 2, and underwent a closed fracture surgery with treatment of either PD0325901 or AZD6244. Mouse fractures were harvested at day 21 and TRAP stained for osteoclasts. Treatment with PD0325901 or AZD6244 led to a significant reduction in osteoclast number and surface in the continuous or late treatment groups (black bars). Treatment in the early group was stopped 11 days before harvest, and the osteoclast levels began to return to normal (gray bars). (*p < 0.05, **p < 0.01, ANOVA, N = 5).

was controlled *via* post-operative i.p. injection with 1 ml sterile saline. Fracture repair was monitored by weekly radiography (Faxitron X-ray) and in the event where internal fixation had failed (due to pin slippage, bending or breakage) the affected mouse was culled and excluded from subsequent analysis. At the experimental endpoints, animals were euthanized using carbon dioxide and specimens collected post-mortem for radiography and histology. All animal experiments were undertaken with approval from the local animal ethics committee.

Treatment with PD0325901 or AZD6244

Mice were single housed prior to the beginning of the experiment, and they were trained to eat a strawberry jelly as drug vehicle. This jelly was composed of 0.8% DMSO (Sigma-Aldrich, St. Louis, MO, USA), 16% Splenda® (Splenda® Low Calorie Sweetener, Johnson-Johnson Pacific Pty, NSW, Australia), 9.6% gelatine (Davis Gelatin, GELITA Australia Pty, NSW, Australia) and 7.9% flavoring (QUEEN Flavoring Essence Imitation Strawberry, Queen Fine Foods Pty, QLD, Australia). The jelly was given to the mice with or without PD0325901 (Selleck Chemicals, TX, USA) or AZD6244 (Chemietek, IN, USA) dissolved in DMSO. This method of administration proved very effective at drug delivery, and reduced the stress normally associated with oral gavage. Single-housing of the mice assured that the jelly was being consumed at the appropriate dose. This method has been previously described [19].

Histological analysis

Fractured tibiae were removed along with the surrounding soft tissues, fixed overnight in 4% paraformaldehyde, and then stored in 70% alcohol at 4 °C prior to decalcification. For growth plate analyses, the contralateral femora were removed and processed in a similar fashion. Bone samples were decalcified in 0.34 M EDTA (pH 8.0) for 21 days at 4 °C on shaker with changes every 2–3 days. Samples were embedded in paraffin blocks and 5 μm-thick sections were cut and stained with Picrosirius Red/Alcian Blue to stain for bone and cartilage, and counterstained with Harris Hematoxylin. Adjacent sections were

Table 2
Blood biochemistry for RANKL and OPG in AZD6244 treated animals.

	RANKL (pg/ml)	OPG (pg/ml)	RANKL/OPG
Day 10			
Vehicle	36.38 (±5.71)	2253.5 (±117)	0.0167
AZD6244	21.08 (±2.52)	2463.5 (±296)	0.0095
Day 21			
Vehicle	98.08 (±6.70)	445447 (±30459)	0.0002
Continuous	73.23** (±4.95)	332510* (±22524)	0.0002
Late	78.54 (5.33)	356636 (±24209)	0.0002
Early	114.59 (±4.87)	520506 (±22126)	0.0002

Mice underwent a fracture surgery and were treated with AZD6244 as described in Fig. 2. Blood was collected at day 10 and day 21 post fractures, and circulating levels of RANKL and OPG were measured. The ratio of RANKL to OPG was also calculated.
** p < 0.01, ANOVA with Dunnett's post-test, N = 5–10.

stained for tartrate-resistant acid phosphatase (TRAP) to highlight osteoclasts, and counterstained with 0.4% Light Green. Stained sections were quantified and analyzed using Bioquant Analysis System (Nashville, TN, USA). One section per biological sample was analyzed, and for histology, the values were normalized to tissue area. These methods have been previously published [17,18].

Serum RANKL and OPG

Blood was collected *via* cardiac puncture of C57/Bl6 animals at the experimental endpoint. Blood was allowed to clot for 30 min at room temperature before centrifugation. The serum was stored at -20 °C. For RANKL and OPG readings, blood samples were freshly thawed and assayed using the RANKL or OPG kits supplied by R&D Systems (Minneapolis, USA).

Sheep articular chondrocyte cultures

Under sterile conditions full depth articular cartilage was removed from the femoral and tibial surfaces of skeletally mature (2–3 year old) ovine knee joints within 6 h of sacrifice. Chondrocytes were isolated by digesting cartilage in 0.1% Pronase (Roche) in Dulbecco's modified Eagle's medium — Nutrient mixture F-12 Ham (DMEM/F12; Sigma) with 10% (v/v) fetal calf serum (FCS; Ausgenex, Brisbane, Australia) for 2 h at 37 °C. Tissue was then washed and digested with 0.05% collagenase (Sigma) in DMEM/F12 with 10% FCS overnight at 37 °C with agitation. Cells were then cultured (replicate cultures for each analytical point) in fresh media with or without interleukin-1-alpha

(IL-1; 1 ng/mL; PeproTech) in the presence or absence of PD0325901 or AZD6244 (1 nM, 100 nM) for 24 h before RNA harvest using Trizol Reagent. This method is previously described [20,21].

qPCR was performed using the following primer sequences: GAPDH: F — CCTGGAGAAACCTGCCAAGTATG, R — GGTAGAAGAGTGAGTG TCGCTGTTG; Collagen 1: F — ATCCCTGGACAACCTGGACTTC, R — TCATCATAGCCGTAAGACAACTGG; Collagen 2: F — TGACCTGACGC CCATTCATC, R — TTTCCTGTCTCTGCCTTGACCC; Aggrecan: F — TCACC ATCCCCTGCTACTTCATC, R — TCTCCTTGGAAATGCGGCTC; ADAMTS-4: F — AACTCGAAGCAATGCACTGGT, R — TGCCCGAAGCCATTGTCTA; ADAMTS-5: F — GCATTGACGCATCCAAACCC, R — CGTGGTAGGTC CAGCAAACAGTTAC; MMP-13: F — GGTGACAGGCAGACTTGATGATAAC, R — ATTTGGTCCAGGAGGGAAAGCG. These primers have been previously validated and result in a single peak on a dissociation curve [17].

Statistical methods

Sample size for each experiment is indicated in the appropriate figure legend. Samples that were larger than two standard deviations were defined as outliers and not included in the analysis. For fracture studies, a Fisher Exact Test was performed based on unions and non-unions for the treatment and untreated groups. For the histological analysis, a one-way analysis of variance was performed, with a Dunnett's or Tukey's multiple comparisons post-test. For quantitative PCR, a *t*-test was used to determine significant between individual genes. All analyses were performed using GraphPad Prism 6 (La Jolla, CA, USA).
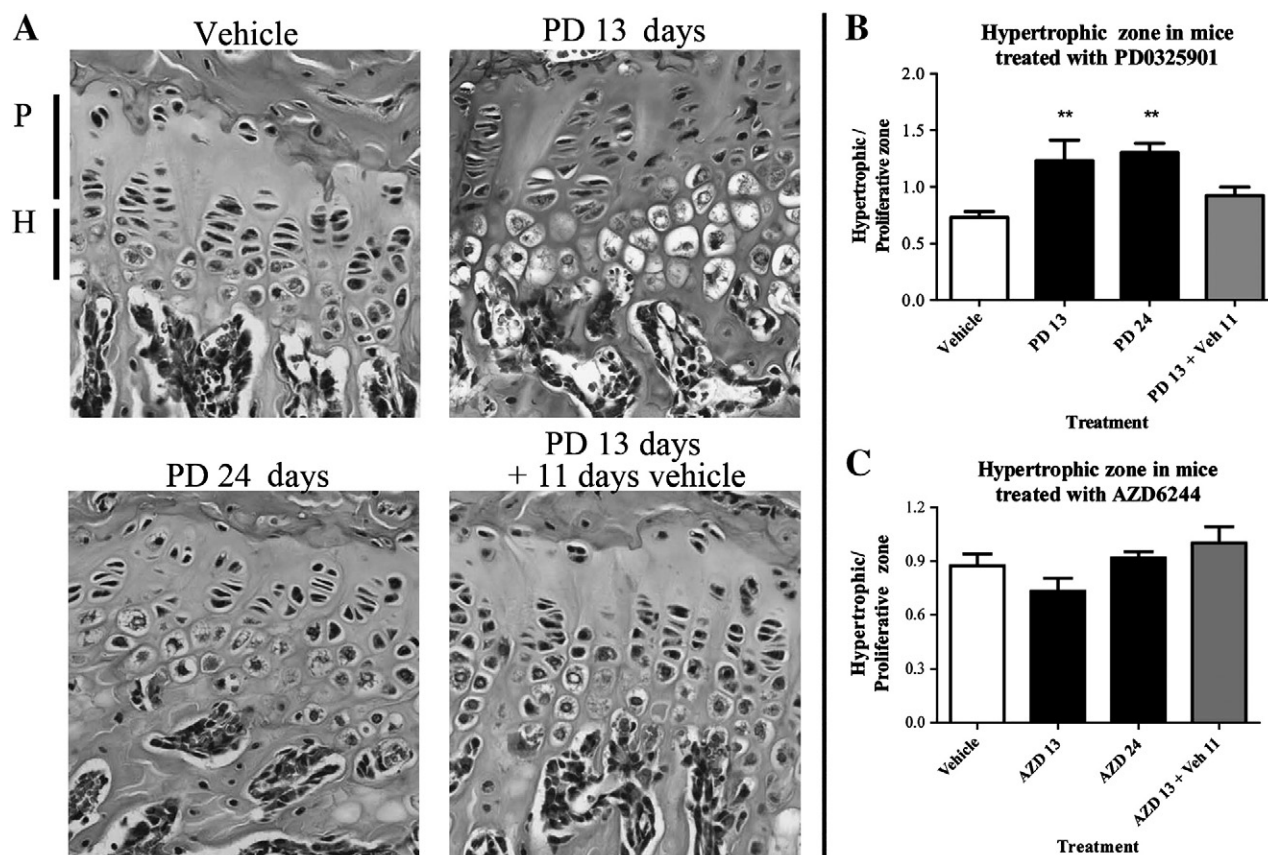

Fig. 6. MEK signaling is essential for normal growth plate development. The femurs from the animals described in Fig. 2 were harvested to determine the impact of MEK inhibition on growth plate dynamics. The growth plate of the mice was stained with Hematoxylin and Eosin, and the length of the hypertrophic (H) over the proliferative (P) zone was compared (A). Drug treatment for 13 or 24 days resulted in an expansion of the hypertrophic zone in PD0325901 treated mice (B), but no change in AZD6244 treated mice (C). The total length of the growth plate was not changed. When mice are taken off PD0325901 for 11 days, the hypertrophic zone began to remodel back to its original length (B, gray bar). (**$p < 0.01$, ANOVA, N = 3–5).

A Gene Expression of *Collagen-1* in Cultured Sheep Chondrocytes with 24 hours of MEKi Treatment

B Gene Expression of *Collagen-2* in Cultured Sheep Chondrocytes with 24 hours of MEKi Treatment

C Gene Expression of *Aggrecan* in Cultured Sheep Chondrocytes with 24 hours of MEKi Treatment

D Gene Expression of *MMP-13* in Cultured Sheep Chondrocytes with 24 hours of MEKi Treatment

E Gene Expression of *ADAMTS-4* in Cultured Sheep Chondrocytes with 24 hours of MEKi Treatment

F Gene Expression of *ADAMTS-5* in Cultured Sheep Chondrocytes with 24 hours of MEKi Treatment

fracture for analysis of the femur, fracture callus, and serum biochemistry. Animals harvested at day 10 post fracture received a total of 13 doses, while animals in the continuous group received 24 doses by day 21 time point.

Fractures were analyzed by microCT 21 days post-fracture to quantify the mineralized bone volume in the fracture callus (Table 1). Continuous treatment with either PD0325901 or AZD6244 resulted in a significant increase in BV/TV (bone volume relative to tissue volume). With PD0325901 the total callus BV (bone volume) was increased, but not significantly so; in AZD6244 treated animals the callus BV showed a 20–23% reduction (p < 0.01), but this was also associated with reductions in (TV) tissue volume of 27–32% (p < 0.05). To further analyze the calluses, detailed histology was assessed at day 10 and day 21 post-fracture.

Day 10 specimens revealed a significantly greater cartilage area when treated with PD0325901 compared to vehicle controls (Fig. 3A). Treatment with AZD6244 also produced a trend towards increased cartilage but this did not reach statistical significance (Fig. 3B). This time point represents the peak cartilage formation step during fracture healing, suggesting early MEKi treatment promoted the accumulation or formation of cartilage. Day 21 specimens similarly showed considerable and statistically significant retention of cartilage with continuous MEKi treatment with either PD0325901 or AZD6244 (Figs. 3C, D). Mice treated with MEKi after the establishment of the cartilaginous soft callus (Late group, days 10–21) showed an increase in the amount of cartilage remaining (Fig. 3). This cartilage appeared characteristically hypertrophic and mineralized (Fig. 4). The effects on cartilage retention of d10–21 treatment were more pronounced with PD0325901 treatment than with AZD6244 (Fig. 3). In contrast, cessation of MEKi treatment after day 10 (Early group, days −3–10) led to negligible residual cartilage remaining by day 21 (Fig. 3). These data indicate that MEK inhibition may impact chondrocyte terminal differentiation and cartilage resorption.

MEK inhibition reduces osteoclastogenesis in the fracture callus

In fracture healing, osteoclasts are critical for remodeling of the hard callus, effects of MEKi on osteoclastogenesis were hypothesized based on cell culture data in vitro. A stain for tartrate-resistant acid phosphatase (TRAP) for osteoclasts was performed and significant effects were seen at 21 days with MEKi treatment. Treatment with PD0325901 (Continuous) resulted in a 43% decrease in osteoclast surface (p = 0.03) (Fig. 5A). These effects were reversible, as PD0325901 (Early) showed no difference. Mice treated with AZD6244 (Continuous) also showed a significant 21% decrease in osteoclast surface (p = 0.005) (Fig. 5C). However, unlike PD0325901 (Early), AZD6244 (Early) showed a persistent decrease even after 11 days (Fig. 5D). This was not associated with significant changes in BV or BV/TV in the bone below the growth plate as measured by microCT (data not shown).

Serum was collected from animals treated with AZD6244 at day 10 and at day 21 post-fracture and analyzed for RANKL and OPG biochemistry. 10 days of treatment with 10 mg/kg of AZD6244 produced a 42% reduction in circulating RANKL (Table 2) and no change in OPG. Intramouse variability was high and this difference did not reach statistical significance. 21 days of AZD6244 treatment led to a statistically significant reduction in RANKL (25%, P < 0.05), but also comparable reduction in OPG. These data suggest the changes in osteoclast surface at the fracture site may reflect differences in the local fracture microenvironment rather than systemic changes in bone resorption.

MEK inhibition maintains hypertrophic chondrocytes at the growth plate

The growth plates from the animals that underwent fracture surgery were also analyzed to help elucidate what stage of cellular differentiation MEKi treatment may influence. The specimens examined were either treated with MEKi for 13 days, 24 days, or 13 days with a wash-out period of 11 days. Growth plates were analyzed by comparison of the proliferative zones and hypertrophic zones. The hypertrophic zone was significantly expanded with 13 or 24 days PD0325901 treatment (Figs. 6A, B). The proliferative zone was correspondingly decreased, leaving the total growth plate length unchanged with treatment. After the 11 day washout period, no difference in hypertrophic zone was seen, suggesting the effects were reversible over the time period studied. In contrast, AZD6244 was not found to significantly affect the growth plate (Fig. 6C).

To determine whether osteoclasts were affected below the growth plate of these animals, a TRAP stain was performed in the primary spongiosa. In mice treated with PD0325901, osteoclast number and surface were significantly reduced after 13 and 24 days, but again was reversible with 11 day washout (Figs. 7A, B). In contrast, the trend towards reduced osteoclast number and surface did not reach significance in animals treated with AZD6244 (Figs. 7C, D) except in 13 day treatment/11 day washout group. This suggests some underlying differences in impact on osteoclasts and reversibility between the two agents.

MEK inhibition affects expression of matrix factors and catabolic enzymes in cultured chondrocytes

Based on the fracture healing and growth plate data, it was hypothesized that the skeletal effects of MEKi may mechanistically involve effects on cartilage matrix production and breakdown. This was further examined in vitro using sheep articular chondrocytes treated with PD0325901 and AZD6244. These cells were selected because they can be induced to strongly increase expression of catabolic enzymes with interleukin treatment.

MEKi treatment with 100 mM PD0325901 and 100 mM AZD6244 led to significant increases in the cartilage-specific matrix genes Collagen-2 (Col2a1) and Aggrecan (Acan). Collagen-1 (Col1a1), a marker of chondrocyte de-differentiation, was not affected by PD0325901 and more modestly increased by 100 mM AZD6244 (Figs. 8A–C). Treatment of chondrocytes with IL-1 resulted in significant decreases in the gene expression of Col1a1, Col2a1, and Acan (Figs. 8A–C). MEKi treatment led to partial rescue of genes encoding matrix proteins, with the most potent effects on Col1a1.

Expression of cartilage degrading enzymes Adamts-4 (a disintegrin and metalloproteinase with thrombospondin motifs-4), Adamts-5, and Mmp13 was quantified. MEK inhibition led to significant decreases in Adamts-5 and Mmp13 expression, even with 1 mM PD0325901 and 1 mM AZD6244 (Figs. 8D–F). Consistent with the articular chondrocyte culture model, 1 ng/ml IL-1 treatment dramatically increased expression of genes encoding these enzymes, in some cases by several orders of magnitude. While Adamts-4/5 expression were unchanged or slightly increased by the MEKi compounds (Figs. 8E–F), Mmp13 expression was significantly decreased (Fig. 8D).

Overall, these data indicate that MEKi compounds can increase the expression of specific cartilage matrix genes while decreasing Mmp13 expression, which would favor the accumulation and retention of cartilage.

Fig. 8. MEKi compounds regulate chondrogenesis. Sheep articular chondrocyte explant cultures were grown for 24 h in the presence of IL-1, PD0325901 (gray bars) or AZD6244 (black bars). mRNA was harvested for quantitative PCR of anabolic makers (A–C; Collagen 1 and 2, Acan, respectively), and catabolic markers (D–F; Mmp13, Adamts-4 and 5, respectively). MEKi treatment consistently increases anabolic markers with or without treatment of IL-1 (A–C). MEKi treatment also inhibited catabolic enzymes when IL-1 was not delivered. Mmp13 was reduced when cells were treated with IL-1 and a MEKi (D). (N = 6, t-test, *p < 0.05 compared to untreated control; τ p < 0.05 compared to IL-1 treatment alone).

Discussion

The effects of MEK inhibition on bone cells

Numerous *in vitro* studies have attempted to evaluate the role of the Ras–MAPK pathway in bone cells, although a clear consensus has not yet been reached [22]. The use of older MEKi compounds such as PD98059 or U0126 have been a useful guide, but these compounds are less specific that PD0325901 or AZD6244 [23,24]. In C2C12 muscle cells and MC3T3 pre-osteoblastic cells, PD98059 were found to promote osteoblastogenesis synergistically with rhBMP2 [25]. Chondrogenic micromass cultures treated with PD98059 or U0126 show increased expression of *Acan* and *Col2a1*, suggesting that they promote chondrogenesis [26]. Our *in vitro* experiments with these highly specific inhibitors indicate that the Ras–MAPK pathway is a negative regulator of osteoblast maturation. MEK inhibition led to a greater relative increase in chondrocyte gene expression markers than in osteoblasts markers. This suggests that chondrocytes are more sensitive to variations in Ras–MAPK activity than osteoblasts.

The effects of MEK inhibition on bone repair

Fracture healing can be temporally divided into an inflammatory phase, a soft callus phase, a hard callus phase, and a remodeling phase, although these stages show some overlap [13]. The bone repair process involves the coordination of multiple cell types to restore normal bone shape and function. Our data reveals that treatment with PD0325901 or AZD6244 can significantly impair the endochondral ossification in a fracture callus. Peak cartilage was increased with PD0325901, cartilage remodeling was decreased, and the number of osteoclasts in the callus was decreased. Treatment with AZD6244 did not result in a significant increase in peak cartilage at day 10, but at day 21, we observed a significant increase in cartilage, suggesting impairment of cartilage resorption. The effects of PD0325901 and AZD6244 treatments were examined by microCT, and differences in bone parameters with MEKi treatment were noted. Based on the histology, it is possible that retention of mineralized cartilage may underlie some of the changes in BV/TV detected using this modality.

Serum samples revealed that the RANKL to OPG ratio was not changed with MEKi treatment, despite a change in osteoclast surface/bone surface. This is likely because RANKL is secreted by osteocytes embedded in the matrix to regulate osteoclasts locally, rather than through systemic osteoclast regulation [27]. While osteoclast surface/bone surface was significantly reduced, we did not observe a significant effect on osteoclast number/bone surface, and this may be due to a lack of statistical power for this parameter (Fig. 5).

The process of cartilage remodeling during endochondral ossification is normally undertaken by osteoclasts as well as other cell types that secrete matrix metalloproteinases (MMPs). Insight into the cells that can participate in endochondral remodeling have been elucidated by several recent studies. Treatment with the MMP inhibitor MM1270 led to the accumulation of cartilage in a rat fracture model. In contrast, treatment with bisphosphonates (which abrogate osteoclast-mediated resorption) or OPG (which blocks osteoclast formation) activity lead to increased bone mineral content due to delayed hard callus remodeling, but no delay in cartilaginous/soft callus remodeling [28]. Analogously, *Mmp9* or *Mmp13* knockout mice that underwent a fracture surgery show delayed cartilage remodeling, and a persistent cartilaginous fracture callus [29,30]. These experiments indicate that the primary mechanism of cartilage remodeling during fracture healing is through the action of MMPs, which can be expressed by a range of cell types and not solely osteoclasts. Critically, our *in vitro* evidence from articular sheep chondrocytes treated with either PD0325901 or AZD6244 showed an inhibition of *Mmp13* expression.

The effects of MEK inhibition on chondrocytes and cartilage

This study is the first to document the effects of either PD0325901 or AZD6244 on the growth plate and during fracture healing. Previous studies have successfully used PD0325901 at 20–50 mg/kg in mouse tumor xenograft models [4,31]. We dosed mice with 10–25 mg/kg using a published oral delivery method that reduces gavage-induced stress [19]. In a dose finding study, we had a 15% death rate after eight day treatment for mice that had undergone a fracture and treated with PD0325901 at 25 mg/kg/day (data not shown). Therefore, we reduced the dose to 10 mg/kg, which has been suggested to be the clinically relevant equivalent in mice for PD0325901, and did not observe any toxicity [32]. We observed an expansion of the hypertrophic zone in the MEKi treated mice, but the overall growth plate length was not changed. Therefore, the hypertrophic zone was expanded at the expense of the proliferative zone, suggesting that proliferative chondrocytes may be prematurely differentiating into hypertrophic chondrocytes. MEK inhibition using U0126 was shown to have direct impacts on hypertrophic chondrocytes. Inhibition of pERK using U0126 was associated with reduced hypertrophic chondrocyte apoptosis in culture, and a concomitant increase in the hypertrophic zone of the growth plate in mice [33]. Notably however, PD0325901 has also been shown to increase serum phosphate levels [34], and this can be associated with increases in hypertrophic chondrocyte apoptosis [33].

Chondrocyte cultures revealed that MEKi could decrease *Mmp13* expression, and this could underlie expansion of the hypertrophic zone. *Mmp9* and *Mmp13* knockout mice are reported to display an expansion of the hypertrophic zone of the growth plate, but this is also accompanied by a longer growth plate [35]. Mechanistic studies have demonstrated that the effects of *Mmp13* at the growth plate are predominantly due to a reduction in matrix turnover, rather than a change in hypertrophic chondrocyte differentiation or apoptosis [36]. Some reductions in osteoclast parameters were noted at the level of the growth plate, but this is unlikely to perturb proliferative or hypertrophic chondrocyte differentiation. In *Rankl*$^{-/-}$ mice that lack osteoclasts, the expansion of the growth plate and hypertrophic zone was associated with reduced matrix turnover, but chondrocyte differentiation was not impacted. As the MEKi treated mice do not show a change in growth plate length, we posit the hypertrophic zone expansion is not primarily caused by direct effects on MMP expression or osteoclasts. Most likely, these effects are secondary to direct effects of MEKi on chondrocyte differentiation.

In summary, we speculate that the impact of PD0325901 on the growth plate may be mediated through (1) premature differentiation of proliferating chondrocytes, (2) direct anti-apoptotic effects on hypertrophic chondrocytes, and (3) a protective effect from serum phosphate levels, which has been reported with PD0325901 [34]. These effects of MEKi treatment on the growth plate and on hypertrophic chondrocytes may warrant further examination in pediatric patients that are being administered these drugs in clinical trials.

Study limitations

Both of these MEKi compounds are currently in clinical development to treat cancer [37–39]. The data presented from this study provide evidence that support an important role for the Ras–MAPK pathway in fracture healing and skeletal remodeling. We showed that PD0325901 and AZD6244 were capable of promoting cartilage formation during fracture healing, and delaying cartilage matrix resorption, resulting in altered endochondral ossification at the growth plate and fracture callus. The *in vitro* data suggests that *MMP-13* inhibition may be the mechanism for delayed cartilage remodeling. The use of two MEK inhibitors at the same dose confirms the specificity of the effects on the MEK pathway, and allows a dosage comparison that is relevant for future studies.

We did not specifically assess angiogenesis, which is also an important process for endochondral ossification that may be affected by MEK

inhibitors. The impact of these compounds on articular cartilage was not assessed either, though the *in vitro* data was highly informative. Finally, the long-term impact of MEKi compounds on the growth plate remains to be evaluated, since our results only reflect three weeks of treatment. The reversibility of the effects is promising, however.

Conclusions

These data demonstrate an important role for MEK signaling in the maintenance of cartilage and in endochondral bone repair. As MEKi compounds progress through clinical trials, evidence about how they impact the skeleton is essential, particularly in growing children or patients who sustain a fracture. Future studies may identify new ways to utilize this new class of drugs to modulate cartilage turnover and differentiation to improve bone and joint health.

Authors' roles

Study design: AS, DGL, CBL, JEH. Study conduct: KM, MK, ND, MTJ, JEH. Data collection: JEH, MTJ. Data analysis: JEH, MTJ. Data interpretation: AS, DGL, CBL, MM, JEH. Drafting of manuscript: JEH. Revising manuscript content: AS, DGL, CBL, MM. Approving final version of manuscript: AS, DGL. JEH takes responsibility for the integrity of the data analysis.

Acknowledgments

References

[1] Prior IA, Lewis PD, Mattos C. A comprehensive survey of Ras mutations in cancer. Cancer Res 2012;72:2457–67.
[2] Davies H, Bignell GR, Cox C, Stephens P, Edkins S, Clegg S, et al. Mutations of the BRAF gene in human cancer. Nature 2002;417:949–54.
[3] Huynh H, Chow PK, Soo KC. AZD6244 and doxorubicin induce growth suppression and apoptosis in mouse models of hepatocellular carcinoma. Mol Cancer Ther 2007;6:2468–76.
[4] Henderson YC, Chen YY, Frederick MJ, Lai SY, Clayman GL. MEK inhibitor PD0325901 significantly reduces the growth of papillary thyroid carcinoma cells in vitro and in vivo. Mol Cancer Ther 2010;9:1968–76.
[5] Koup JR, Liu J, Loi C-M, Howard C, Van Becelaere K, Przybranowski S, et al. PK/PD modeling of biomarker (p-ERK) response and tumor growth to PD 0325901 in a human tumor xenograft mouse model. AACR meeting abstracts 2004; 2004. p. 1248-b-.
[6] Denton CL, Gustafson DL. Pharmacokinetics and pharmacodynamics of AZD6244 (ARRY-142886) in tumor-bearing nude mice. Cancer Chemother Pharmacol 2011;67:349–60.
[7] Adjei AA, Cohen RB, Franklin W, Morris C, Wilson D, Molina JR, et al. Phase I pharmacokinetic and pharmacodynamic study of the oral, small-molecule mitogen-activated protein kinase kinase 1/2 inhibitor AZD6244 (ARRY-142886) in patients with advanced cancers. J Clin Oncol 2008;26:2139–46.
[8] Guise TA. Bone loss and fracture risk associated with cancer therapy. Oncologist 2006;11:1121–31.
[9] Kanis JA, McCloskey EV, Powles T, Paterson AH, Ashley S, Spector T. A high incidence of vertebral fracture in women with breast cancer. Br J Cancer 1999;79:1179–81.
[10] Lefebvre V, Smits P. Transcriptional control of chondrocyte fate and differentiation. Birth Defects Res C Embryo Today 2005;75:200–12.
[11] Goldring MB, Tsuchimochi K, Ijiri K. The control of chondrogenesis. J Cell Biochem 2006;97:33–44.
[12] Einhorn TA. The cell and molecular biology of fracture healing. Clin Orthop Relat Res 1998:S7-21.
[13] Schindeler A, McDonald MM, Bokko P, Little DG. Bone remodeling during fracture repair: the cellular picture. Semin Cell Dev Biol 2008;19:459–66.
[14] Ge C, Xiao G, Jiang D, Franceschi RT. Critical role of the extracellular signal-regulated kinase–MAPK pathway in osteoblast differentiation and skeletal development. J Cell Biol 2007;176:709–18.
[15] Matsushita T, Chan YY, Kawanami A, Balmes G, Landreth GE, Murakami S. Extracellular signal-regulated kinase 1 (ERK1) and ERK2 play essential roles in osteoblast differentiation and in supporting osteoclastogenesis. Mol Cell Biol 2009;29:5843–57.
[16] Provot S, Nachtrab G, Paruch J, Chen AP, Silva A, Kronenberg HM. A-Raf and B-Raf are dispensable for normal endochondral bone development, and parathyroid hormone-related peptide suppresses extracellular signal-regulated kinase activation in hypertrophic chondrocytes. Mol Cell Biol 2008;28:344–57.
[17] El-Hoss J, Sullivan K, Cheng T, Yu NYC, Bobyn JD, Peacock L, et al. A murine model of neurofibromatosis type 1 tibial pseudarthrosis featuring proliferative fibrous tissue and osteoclast-like cells. J Bone Miner Res 2012;27:68–78.
[18] Schindeler A, Morse A, Harry L, Godfrey C, Mikulec K, McDonald M, et al. Models of tibial fracture healing in normal and Nf1-deficient mice. J Orthop Res 2008;26:1053–60.
[19] Zhang L, Lee NJ, Nguyen AD, Enriquez RF, Riepler SJ, Stehrer B, et al. Additive actions of the cannabinoid and neuropeptide Y systems on adiposity and lipid oxidation. Diabetes Obes Metab 2010;12:591–603.
[20] Little CB, Ghosh P. Variation in proteoglycan metabolism by articular chondrocytes in different joint regions is determined by post-natal mechanical loading. Osteoarthritis Cartilage 1997;5:49–62.
[21] Jackson MT, Smith MM, Smith SM, Jackson CJ, Xue M, Little CB. Activation of cartilage matrix metalloproteinases by activated protein C. Arthritis Rheum 2009;60:780–91.
[22] Schindeler A, Little DG. Ras–MAPK signaling in osteogenic differentiation: friend or foe? J Bone Miner Res 2006;21:1331–8.
[23] Brown A, Carlson T, Loi C-M, Graziano M. Pharmacodynamic and toxicokinetic evaluation of the novel MEK inhibitor, PD0325901, in the rat following oral and intravenous administration. Cancer Chemother Pharmacol 2007;59:671–9.
[24] Yeh TC, Marsh V, Bernat BA, Ballard J, Colwell H, Evans RJ, et al. Biological characterization of ARRY-142886 (AZD6244), a potent, highly selective mitogen-activated protein kinase kinase 1/2 inhibitor. Clin Cancer Res 2007;13:1576–83.
[25] Higuchi C, Myoui A, Hashimoto N, Kuriyama K, Yoshioka K, Yoshikawa H, et al. Continuous inhibition of MAPK signaling promotes the early osteoblastic differentiation and mineralization of the extracellular matrix. J Bone Miner Res 2002;17:1785–94.
[26] Bobick BE, Kulyk WM. The MEK–ERK signaling pathway is a negative regulator of cartilage-specific gene expression in embryonic limb mesenchyme. J Biol Chem 2004;279:4588–95.
[27] Xiong J, Onal M, Jilka RL, Weinstein RS, Manolagas SC, O'Brien CA. Matrix-embedded cells control osteoclast formation. Nat Med 2011;17:1235–41.
[28] McDonald MM, Morse A, Mikulec K, Peacock L, Baldock PA, Kostenuik PJ, et al. MMP driven endochondral fracture union proceeds independently of osteoclast activity. J Bone Miner Res 2013;28:1550–60.
[29] Colnot C, Thompson Z, Miclau T, Werb Z, Helms JA. Altered fracture repair in the absence of MMP9. Development 2003;130:4123–33.
[30] Kosaki N, Takaishi H, Kamekura S, Kimura T, Okada Y, Minqi L, et al. Impaired bone fracture healing in matrix metalloproteinase-13 deficient mice. Biochem Biophys Res Commun 2007;354:846–51.
[31] Ciuffreda L, Del Bufalo D, Desideri M, Di Sanza C, Stoppacciaro A, Ricciardi MR, et al. Growth-inhibitory and antiangiogenic activity of the MEK inhibitor PD0325901 in malignant melanoma with or without BRAF mutations. Neoplasia 2009;11:720–31.
[32] Jessen WJ, Miller SJ, Jousma E, Wu J, Rizvi TA, Brundage ME, et al. MEK inhibition exhibits efficacy in human and mouse neurofibromatosis tumors. J Clin Invest 2013;123:340–7.
[33] Miedlich SU, Zalutskaya A, Zhu ED, Demay MB. Phosphate-induced apoptosis of hypertrophic chondrocytes is associated with a decrease in mitochondrial membrane potential and is dependent upon ERK1/2 phosphorylation. J Biol Chem 2010;285:18270–5.
[34] Ranch D, Zhang MYH, Portale AA, Perwad F. Fibroblast growth factor 23 regulates renal 1,25-dihydroxyvitamin D and phosphate metabolism via the MAP kinase signaling pathway in Hyp mice. J Bone Miner Res 2011;26:1883–90.
[35] Stickens D, Behonick DJ, Ortega N, Heyer B, Hartenstein B, Yu Y, et al. Altered endochondral bone development in matrix metalloproteinase 13-deficient mice. Development 2004;131:5883–95.
[36] Little CB, Barai A, Burkhardt D, Smith SM, Fosang AJ, Werb Z, et al. Matrix metalloproteinase 13-deficient mice are resistant to osteoarthritic cartilage erosion but not chondrocyte hypertrophy or osteophyte development. Arthritis Rheum 2009;60:3723–33.
[37] Kirkwood JM, Bastholt L, Robert C, Sosman J, Larkin J, Hersey P, et al. Phase II, open-label, randomized trial of the MEK1/2 inhibitor selumetinib as monotherapy versus temozolomide in patients with advanced melanoma. Clin Cancer Res 2012;18:555–67.
[38] Wang JY, Wilcoxen KM, Nomoto K, Wu S. Recent advances of MEK inhibitors and their clinical progress. Curr Top Med Chem 2007;7:1364–78.
[39] Boasberg PD, Redfern CH, Daniels GA, Bodkin D, Garrett CR, Ricart AD. Pilot study of PD-0325901 in previously treated patients with advanced melanoma, breast cancer, and colon cancer. Cancer Chemother Pharmacol 2011;68:547–52.